Toxicology 502 (2024) 153715

Contents lists available at ScienceDirect

Toxicology

journal homepage: www.elsevier.com/locate/toxicol

Are the BPA analogues an alternative to classical BPA? Comparison between 2D and alternative 3D in vitro neuron model to assess cytotoxic and genotoxic effects

Marta Sendra [a,b,*], Mónica Cavia-Saiz [a], Pilar Múñiz [a]

[a] Department of Biotechnology and Food Science, Faculty of Sciences, University of Burgos, Plaza Misael Bañuelos, 09001 Burgos, Spain
[b] International Research Center in Critical Raw Materials for Advanced Industrial Technologies (ICCRAM), R&D Center, Universidad de Burgos, Plaza de Misael Bañuelos s/n, 09001 Burgos, Spain

ARTICLE INFO

Keywords:
Toxicology
BPA analogues
Recovery assays
SH-SY5Y 3D model
Alternative in vitro model

ABSTRACT

BPA is used in a wide range of consumer products with very concern toxicological properties. The European Union has restricted its use to protect human health. Industry has substituted BPA by BPA analogues. However, there is a lack of knowledge about their impacts. In this work, BPA and 5 BPA analogues (BPS, BPAP, BPAF, BPFL and BPC) have been studied in classical SH-SY5Y and the alternative 3D in vitro models after 24 and 96 h of exposure. Cell viability, percentage of ROS, cell cycle phases as well as the morphology of the spheroids were measured. The 2D model was more sensitive than the 3D models with differences in cell viability higher than 60% after 24 h of exposure, and different mechanisms of ROS production. After chronic exposure, both models were more affected in comparison to the 24 h exposure. After a recovery time (96 h), the spheroids exposed to 2.5–40 μM were able to recover cell viability and the morphology. Among the BPs tested, BPFL>BPAF>BPAP and >BPC revealed higher toxicological effects, while BPS was the only one with lower effects than BPA. To conclude, the SH-SY5Y 3D model is a suitable candidate to perform more reliable in vitro neurotoxicity tests.

1. Introduction

The 2,2-bis(4-hydroxyphenyl)propane (BPA) is a chemical compound formed by two phenol rings (Barber, 2013) used in plastic and epoxy resin production (BPA) at a rate of 7.7 million tons per year (Czarny-Krzymińska et al., 2022). Currently, BPA is known as an endocrine disruptor and its use has been limited by the EU from 2017 (EFSA EMA, 2023). The Ingested Toxic Dose (ITD) was set at 0.2 nanograms per kilogram of body weight per day (EFSA EMA, 2023). Nowadays, the ITD is more restrictive than in it was in 2015 (4 micrograms per kilogram of body weight per day) due to its negative effects on human health such as: neurotoxicity, immunotoxicity, metabolic disorder, and reproductive disorders (Ma et al., 2019).

The exposure pathways of BPA are the gastrointestinal, respiratory, and dermal tracts through food and water, air and dust, thermal paper, dental materials, and occupational exposure (Liu et al., 2019). BPA has been detected in biological matrices such as serum, plasma, urine, saliva, hair, amniotic fluid, umbilical cord blood, etc. (Liu et al., 2019; Lv et al., 2016; Ma et al., 2019). Furthermore, BPA can cross the blood–brain barrier (Sun et al., 2002) and influence the function and behaviour of the brain (Ma et al., 2019; Sevastre-Berghian et al., 2022). The ratio of the area under the concentration–time curve of BPA in a rat's brain to that in the blood was estimated to be about 3.0–3.8% (Sun et al., 2002).

Recent studies have shown that prenatal exposure to BPA induces neuropsychiatric deficits during childhood, such as depression and anxiety, as well as the social and cognition dysfunction observed in autism spectrum disorder (Miodovnik et al., 2011; Perera et al., 2016) and learning and memory (Li et al., 2023). In addition, exposure to BPA is associated with neurodegeneration due to oxidative stress, neural inflammation, and synaptic dysfunction (Ni et al., 2021; Perera et al., 2016; Pradhan et al., 2023; Rezg et al., 2014; Takahashi et al., 2018). Recently, Pradhan et al., (Pradhan et al., 2023) showed that BPA exposure in zebrafish is associated with the genesis of an aggressive neurobehavioral response. Further, the brain's MAO activity, oxidative stress and chromatin condensation increased with a longer duration of exposure (Pradhan et al., 2023). BPA exposure can also produce cognitive deficits in mice by impairing neurite outgrowth (Bi et al.,

* Corresponding author at: Department of Biotechnology and Food Science, Faculty of Sciences, University of Burgos, Plaza Misael Bañuelos, 09001 Burgos, Spain.
E-mail address: msendra@ubu.es (M. Sendra).

https://doi.org/10.1016/j.tox.2023.153715
Received 30 November 2023; Received in revised form 25 December 2023; Accepted 27 December 2023
Available online 9 January 2024

2022). In relation to in vitro exposure, the exposure of cortical pyramidal neurons from mice to BPA (primary neuronal culturing from E15 mice) reduced the size and number of dendrites and spines; as well as the density of excitatory synapses (Hyun et al., 2022).

Due to the negative effects provoked by BPA in humans and the ecosystem, the EU has limited the amount of BPA in products. Currently, more than 200 BPA analogues have been recorded in industry (Lucarini et al., 2020). Some of the most common BPA analogues used are: BPS, BPAP, BPAF, BPFL and BPC among others (González et al., 2020; Thoene et al., 2018). Despite these BPA analogues already being used in commercial products, there is a lack of knowledge about their toxicity.

It has been observed in the literature that many BPA analogues already used by industry are not only endocrine disruptors, but also have harmful genotoxic effects by inducing breaks in DNA strands, affecting the cell cycle, and cell proliferation, altering the expression of genes involved in DNA damage response and repair, and causing many other changes in cellular functions (Fic et al., 2013; Hercog et al., 2019; Ikhlas et al., 2019; Lee et al., 2017; Sendra et al., 2023; Štampar et al., 2023).

Most of the studies about the toxicity of BPA analogues have been performed in classical (2D) in vitro assays. This kind of classical in vitro assay has a low expression of enzymes, xenobiotic receptors (Štampar et al., 2021, 2019), therefore this in vitro model is not comparable with the functioning of an organ or tissue in vivo and may result in inaccurate and false-positive results (Gerets et al., 2012). A more relevant kind of in vitro model; a 3D model is also being applied in toxicological studies for this reason. 3D models, unlike 2D monolayer cell cultures, can be used for long periods of time to study chronic effects or even in recovery assays after chemical exposure (Bell et al., 2016; Eilenberger et al., 2019; Pfuhler et al., 2020; Štampar et al., 2022).

The main aim of this work is to study the short-term (24 h) and long-term (96 h) toxicity of BPA and 5 BPA analogues; as well as the recovery status in a differentiated 3D in vitro model of human neurons (SH-SY5Y cell line). Moreover, the results concerning the effects provoked by BPA analogues and examined in 2D and 3D neuron models are compared in this study.

2. Materials and methods

2.1. SH-SY5Y differentiated cell line and spheroid formation

The SH-SY5Y human neuroblastoma cell line (ATCC HTB-11) was purchased from ATCC (CRL2266™). The cells were grown in DMEN/F12 cell culture supplemented with FBS (10%), pen/strep (100 IU·mL^{-1}) and 0.2% amphotericin at 37 °C and 5% of CO_2. 3D models or spheroid formations were created by the forced flotation method (Štampar et al., 2019). Briefly explained, the spheroids were formed with an initial cell density of 9000 cells per spheroid with 4% Methocel® A4M in a low-adhesion U-shaped 96-well plate. Both the spheroids and 2D cultures were differentiated with retinoic acid at 5 μM for the first two days and PMA at 80 nM for the next two days (Fig. 1A.1 and A.2). To verify the correct differentiation to neurons, immunofluorescence labelling was performed. That is, the cells were fixed with 4% paraformaldehyde (PFA), blocked for 1 h in PBS with 0.1% saponin and 2% bovine serum albumin (BSA), and then incubated overnight at 4 °C with the polyclonal anti-beta III Tubulin antibody (a neuronal marker; ab18207; 1:500) labelled with Alexa Fluor 488, the antibodies were diluted in a staining buffer (0.1% saponin and 0.1% BSA in PBS). The slides were washed twice with PBS. After washing, the samples were stained with DAPI at a concentration of 1 μg·mL^{-1} for nuclear localization. The samples were mounted using ProLong Antifade reagents (Life Technologies), and pictures were taken with a Leica LASX microscope with 5x and 10x objective and blue (DAPI) and green (neuronal marker); and orange excitation lasers (Fig. 1A.2).

Cell viability was studied with Propidium Iodide (PI) to verify that both the 2D and 3D models were viable throughout the differentiation and time of the experiment. The cells (2D), or spheroids (3D), were washed with PBS and then incubated for 5 min at 37 ºC and in the dark with PI at 10 μg·mL^{-1} in a DMEN/F12 medium without supplements. The cells were washed with PBS and suspended (2D or 3D) in 200 μL of non-supplemented medium, to study either by flow cytometry (2D) or fluorescence microscopy (3D). For the flow cytometry study, the Cytoflex SRT flow cytometer (Beckman Coulter, Miami, FL, USA) was used. The data were analyzed using the CytExpert Srt software (Beckman Coulter, Miami, FL, USA). It was used to study the percentage of the population positive for PI (non-viable cells). The excitation of the PI in the 3D models was carried out using a 488 nm laser and the emission detector was set at 585/42. Significant changes ($p < 0.05$) were observed 8 days after culture in the 2D models, although they were not higher than 15% of the total population. In relation to the spheroids, the viability and area was recorded during the exposure time (8 days) and the recovery experiments (12 days); Fig. 1B.

The viability of the spheroids was analysed using fluorescence microscopy in the Leica LASX microscope with the 5x objective and the orange excitation laser. A z-stack of 20 plans was created for image analysis of both the area of viable and non-viable cells. The pictures were analysed using ImageJ Software. The spheroids did not show significant differences in the non-viable cells with respect to the total number of spheroids during the entire experiment. However, this area increased significantly ($p < 0.05$) after the recovery assays (although this area was lower than 1%). In relation to the analysis of the area, a decrease was revealed at day 2 due to a closer and more compact interaction between the cells that formed it. In both the 2D and 3D models, $n = 6$ was used to study cell viability.

2.2. Toxicological assays with 2D and 3D SH-SY5Y cell lines

2.2.1. Experimental conditions

The tests were carried out in two types of in vitro models; 2D and 3D, in order to observe the differences between both models. The 2D assays were run in flat-bottomed 96-well plates with an initial cell density of 30,000 cells per well, while the 3D assay was performed in U-bottomed 96-well plates in which the initial cell density was of 9000 cells per spheroid and well. All the exposure tests were subjected to two periods of time, one of 24 h (short-term) and the other of 96 h (long-term) to observe acute and chronic effects in vitro. The bisphenols used in the exposure assays were: Bisphenol A (4,4′-(propano-2,2-diil) diphenol; BPA; 80–05-7), Bisphenol S (4,4′-Sulfonildiphenol; BPS; 80–09-1), Bisphenol AP (4,4′-(1-feniletiliden) bisfenol; BPAP; 1571–75-1), Bisphenol AF (4,4´- (Hexafluoroisopropiliden) diphenol; BPAF; 1478–61-1), Bisphenol FL (9,9-Bis (4-hidroxifenil) fluorene; BPFL; 3236–71-3) y Bisphenol C (4,4′-(2,2-dicloroetane-1,1-diil) diphenol; BPC; 14868–03-2). The concentrations used of the BPs increased from 2.5 to 160 μM (2.5, 5, 10, 40, 80 and 160) and the control samples contained DMSO solvent control (employing the same percentage used in the highest concentration of the study). During the exposure experiments the culture media with the chemical compounds were replaced every 48 h.

The recovery assays were performed only in the 3D model over 96 h after the exposure time to study the recovery of spheroid viability and area. In the recovery assays the culture media without BPs were replaced every 48 h.

2.2.2. Cytotoxic effects of the bisphenols determined by the MTT assay

A standardised protocol was followed to carry out this assay. The protocol is as follows, MTT is added at a concentration of 5 mg·mL^{-1} to each sample and incubated in the dark at 37 ºC and 5% CO_2 for 2 h. The medium is removed after this incubation and 100 μL of DMSO is added to each well. In the case of the 3D models, the spheroids were moved to 96 flat-bottomed well plates before MTT incubation. The spheroids must disaggregate after incubation. A control of solvent with DMSO and a positive control with 17 μM of etoposide were recorded in parallel in each plate. Absorbance was measured at 570 nm using a multireader

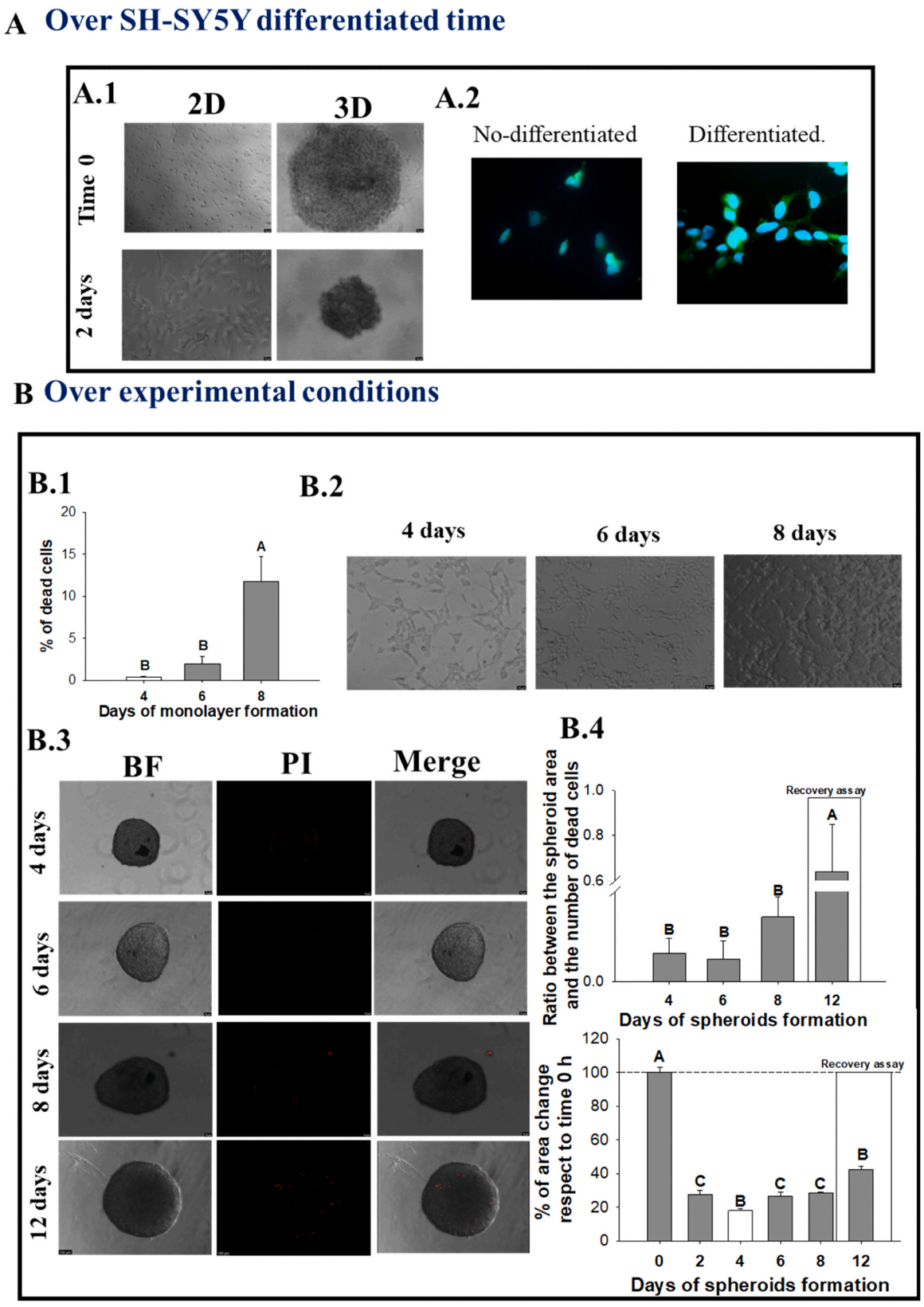

Fig. 1. 2D and 3D SH-SY5Y in vitro models over differentiation, BPs exposure and recovery assays. In the Panel A is observed 2D and 3D models under differentiation with retinoic acid and PMA, as well as immunochemistry images with anti-beta III Tubulin antibody (neuronal marker; green) and DAPI (nuclear marker; blue). In the Panel B is showed the cell viability in 2D model by flow cytometry and 3D model by microscopy; as well as planimetry study.

(Tecan; SPARK®). The MTT assays were performed during the exposure and recovery assays, n = 4 independent experiments. Data were represented as a percentage of cell viability with respect to the DMSO controls.

2.2.3. Surface area of the spheroids

The area of spheroids was studied after the exposure (24 and 96 h) and the recovery experiments. Ten spheroids from 3 independent experiments were photographed using a Leica LASX microscope at 5x objective. The program used to carry out this analysis was ImageJ, where the change in area was compared as a percentage of change with respect to the controls.

2.2.4. Reactive Oxygen Species (ROS) analysis

ROS analyses were performed for the 2D and 3D models at 24 and 96 h for the 6 BPs at 2.5, 10, 40, 80 and 160 μM, as well as for the control of DMSO and etoposide at 17 μM as the positive control. For the ROS analysis, the 2D and 3D models were incubated with DCFH-DA at 20 μM for 30 min. After this time, the 2D and 3D cultures were washed with PBS and re-suspended in 200 μL of DMEN/F12 without supplementation to analyse the percentage of ROS by flow cytometry; CytoFlex SRT; (488 nm excitation laser; 520 nm emission detector) with respect to the total population for the 2D experiments and fluorescence microscopy (488/525; ex/em) for the 3D ones. For 3D, the mean fluorescence of the spheroid area was studied using ImageJ software and represented as the percentage change in fluorescence from the mean fluorescence of the solvent controls. A n = 4 was employed in the different experiments for this study.

2.2.5. Cell cycle analysis

The study of the cell cycle was studied in the 2D and 3D models at 24 and 96 h at a concentration of 1 μM. This concentration was used because 2.5 μM triggered significant decrease in the endpoints previously mentioned for the BPs tested with n = 3 (in each n:8 spheroids were collected per replicate) for each respective bisphenol. For the 2D assays, the samples were collected and centrifuged at 100 g for 5 min. For both in vitro models, the cells were washed with PBS, and fixed with 4% PFA for 20 min. After fixing the cells, they were washed with PBS and re-suspended in it. In the case of the 3D models, the spheroids were collected, centrifuged and disintegrated using a collagenase:trypleE solution in a 1:2 ratio. Once disintegrated, they were fixed using the same procedure used for the 2D assays.

For nuclear staining, the cells were stained with DAPI at a concentration of 1 $\mu g \cdot mL^{-1}$ for 10 min in a solution of 0.1% tritonX-100 in PBS to permeabilise the cells. The cells were centrifuged and re-suspended in 200 μL of PBS for subsequent analysis by flow cytometry after staining. The violet laser was used to excite the DAPI and the detector 450/45 in the flow cytometer. The percentages of G0/G1, S and G2 were studied in the cell population identified and percentages of cells in G1, S, and G2/M phases were analyzed using CytoFlex SRT software. For this study was employed a n = 3 in different experiments.

2.2.6. Statistical analysis

Data analysis was carried out using the Sigmaplot 11 program. The statistical difference between treatments and controls was evaluated by means of an ANOVA statistical analysis with Dunnett and Tukey's post-Hoc, according to the endpoint studied (asterisks (*) mean $p < 0.05$). The comparison between the two models, 2D and 3D, was carried out using a t-test to analyse any significant differences between them ($p < 0.05$ is represented with #).

3. Results

3.1. The effects of BPA and its analogues on the viability of the 2D and 3D in vitro models

The cell viability of the 2D and 3D models of the SH-SY5Y cell line was analysed using the MTT assay after exposure to the selected BPs for 24 and 96 h; Fig. 2A.

In relation to the **acute toxicity tests** (Fig. 2A), the results showed a significant, dose-dependent decrease in the 2D model at both 24 and 96 h. The cell viability showed a significant decrease in the cultures exposed to BPAP, BPAF and BPFL from the concentration of 5 μM ($p < 0.05$). At 24 h of exposure in the 2D models, only BPA produced significant changes; 74.43 ± 1.72%; for the highest concentration ($p < 0.05$). In the 2D models exposed to BPS, viability slowly decreased to values of approximately 75% from 10 to 160 μM ($p < 0.05$). In relation to the cells exposed to BPAP, BPAF and BPFL, viability was reduced to values of 24.25 ± 2.59, 17.8 ± 0.64 and 17.47 ± 0.88% 160 μM, respectively ($p < 0.05$). Only at low and intermediate concentrations (2.5, 5 and 10 μM) were significant decreases evident during exposure to BPC, reaching values of 65.66 ± 12.32% ($p < 0.05$).

In relation to the 3D models, for the acute tests (24 h), BPA, BPAF and BPFL increased the viability of the spheroid, showing a significant increase ($p < 0.05$) with values of 121.96 ± 7.59, 122.49 ± 4.97 and 134.53 ± 21.67% at concentrations of 40 μM for BPA and BPFL and 160 μM for BPAF respectively. The spheroids exposed to BPS and BPC did not show significant changes for any of the concentrations tested at 24 h ($p > 0.05$). However, there were differences from concentration 5 to 80 μM for BPAP, reaching values of between 70–80% compared to the control ($p < 0.05$). When the two models (2D vs 3D) were compared after 24 h of exposure, significant differences were observed between them ($p < 0.05$). It was confirmed that the spheroids tended to increase their viability compared to the control, while the monolayer culture decreased its viability significantly when exposed to the BPs selected.

In relation to the **chronic toxicity test** (96 h); Fig. 2A. The 2D models presented significant differences between the treatments and controls. The treatments that indicate, the highest sensitivity were BPFL>BPAF>BPAP>BPC with values that reached 5% of viability for the highest concentrations ($p < 0.05$). When the viability of the 3D models was studied under 96 h of exposure, a significant decrease was observed between the controls and the spheroids exposed to BPs ($p < 0.05$). Treatments (BPFL>BPAF>BPAP<BPC) were found to cause a drop in cell viability below 30%. In the case of exposure to BPA and BPS, values of 51.60 ± 17.85% of cell viability were found for the highest concentration of BPA ($p < 0.05$); while the exposure to BPS did not indicate any significant changes ($p > 0.05$). The comparison between both models (2D vs 3D) at 96 h showed significant differences for BPAP, BPAF, BPFL and BPC exposure, showing a difference greater than 20–30% between the 2D and 3D models for BPA, BPAP, BPAF, BPFL and BPC.

In relation to the 3D model **recovery tests** (Fig. 2B), after 96 h without BPs, a significant increase in cell viability respect to chronic exposure test was observed. A total recovery was found for the spheroids that had been exposed to BPA. Spheroids recovering from BPC showed an increase in cell viability higher than 35% respect to 96 h of BPs exposure. Furthermore, the recovery rate for cell viability after exposure to BPAP, BPAF and BPFL was more than 20%.

3.2. The effects of BPA and its analogues on the surface area of the SH-SY5Y spheroids

The area of the spheroids was studied at 24 and 96 h after exposure to the BPs; Figs. 3A and 4A.

In the spheroids exposed to BPs after 24 h in the **acute tests**, a significant increase in the area of the spheroids exposed to BPAP and BPC was only found at the highest concentration ($p < 0.05$); while the

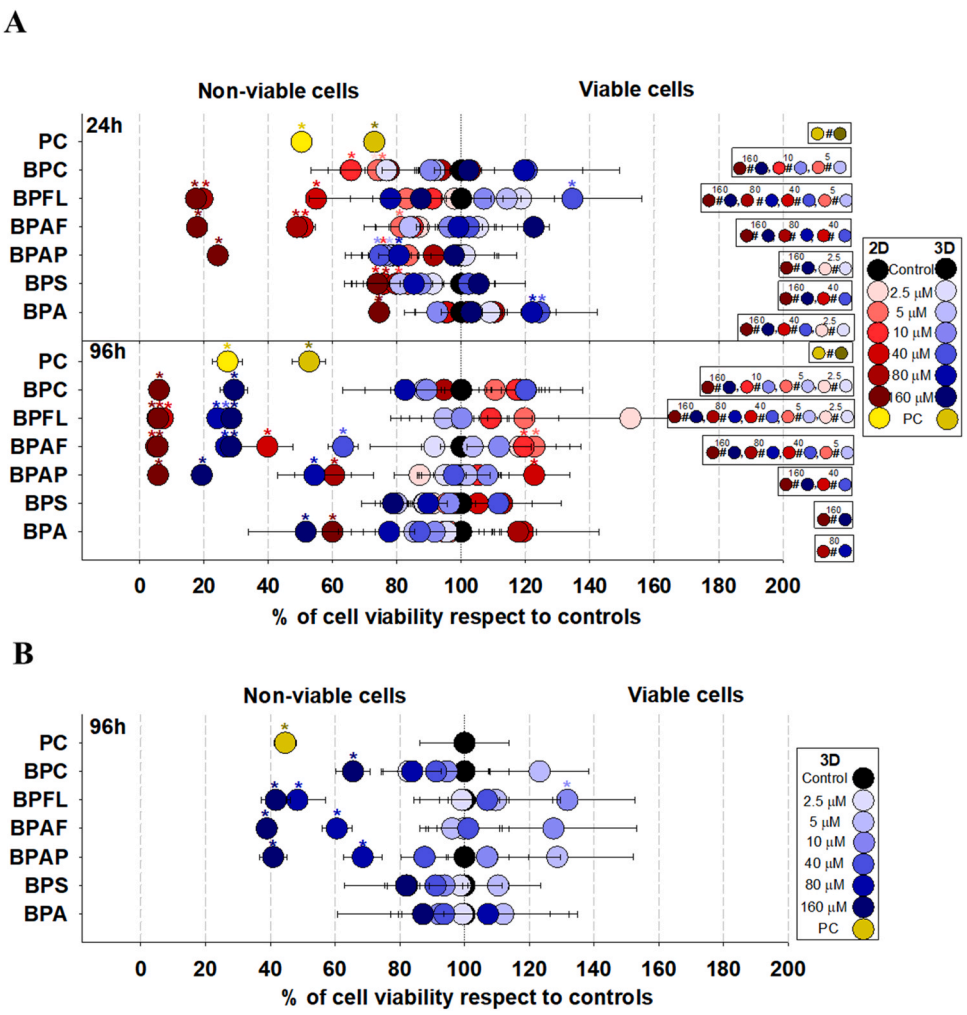

Fig. 2. Percentage of cell viability over the BPs exposure time for 2D and 3D models (panel A) and over recovery assays for 3D models (Panel B). Positive control was etoposide at 17 µM. Differences between controls and concentrations of BPs ($p < 0.05$) was analysed by ANOVA with a Dunnett post-hoc (represented with *). Differences between each in vitro model was study by T-student test (represented with #).

spheroids exposed to BPFL showed a significant decrease in their area when they were exposed to 5–160 µM ($p < 0.05$).

Regarding the **chronic tests** (96 h), BPS was the only treatment that did not show any significant differences in the area with respect to the control ($p > 0.05$). The spheroids exposed to BPA showed a significant decrease in the area with a reduction in the area of 56.37 ± 22.68 and 35.3 ± 18.3% for 80 and 160 µM respectively. The spheroids exposed to BPAP decreased significantly in area for concentrations of 2.5 and 160 µM with values of 68.96 ± 13.76 and 52.76 ± 11.03% ($p < 0.05$). Differences were observed for the concentrations of 2.5, 5, 10, 80 and 160 µM, the first three was around 70% and the other two around 50% and 15% compared to the controls ($p < 0.05$), for the spheroids exposed to BPAF for 96 h. Regarding the BPFL treatment, a clear decrease in area was irrefutably observed, the 80 and 160 µM concentrations showed values of 12.41 ± 5.83 and 34.45 ± 34.14% ($p < 0.05$). The spheroids treated with BPC significantly decreased ($p < 0.05$) at 2.5, 5, 10, 80 and 160 µM to values lower than 70% with respect to the controls.

With regard to the **recovery tests,** only the spheroids exposed to BPA and BPC were able to recover part of their areas in relation to those of the controls. However, the spheroids which were exposed to BPAP, BPAF and BPFL for 96 h totally disintegrated at the highest concentration while those exposed to BPFL totally disintegrated at 80 and 160 µM; Figs. 3B and 4B. Although the spheroids disintegrated at the highest concentration, the other concentrations showed a recovery in relation to the chronic exposure test ($p < 0.05$). Furthermore, the spheroids exposed to BPAP (2.5 µM) and BPAF (2.5 and 5 µM) showed a significant increase in their area in comparison to the controls ($p < 0.05$).

3.3. The effects of BPA and its analogues on the percentage of ROS in the 2D and 3D in vitro models

The percentage of ROS was studied in the 2D and 3D SH-SY5Y models after 24 and 96 h of exposure to concentrations of 2.5, 10, 40, 80 and 160 µM; of the BPs. Fig. 5.

After the **acute toxicity tests** (24 h of exposure to BPs), significant increases ($p < 0.05$) were observed in the 2D models in relation to the 3D models exposed to BPS (160 µM), BPAP (10, 40 and 80 µM), BPAF (40 and 80 µM), BPFL (2.5, 10 and 40 µM) and BPC (2.5, 10, 40, 80 and 160 µM). During the first 24 h of exposure to the BPs for the 2D models, the data showed significantly high values of ROS compared to the controls. Only the monolayer cultures exposed to BPA showed a significant decrease of 62.6 ± 7.7 and 63.7 ± 9.6% at concentrations of 80 and 160 µM compared to the control ($p < 0.05$). BPS produced a significant increase in ROS at 160 µM with a value of 147.08 ± 27.05% compared to the control ($p < 0.05$). Regarding BPAP, a significant increase was noted in the 2D model ($p < 0.05$) at concentrations of 10, 40 and 80 µM, whose values were 371.93 ± 103.96, 211.54 ± 48.95 and 424.4 ± 89.16%, respectively. The highest concentration (160 µM) led to a significant decrease to a value of 38.83 ± 6.24% ($p < 0.05$). The 2D models exposed to BPAF showed an increase in ROS at concentrations of

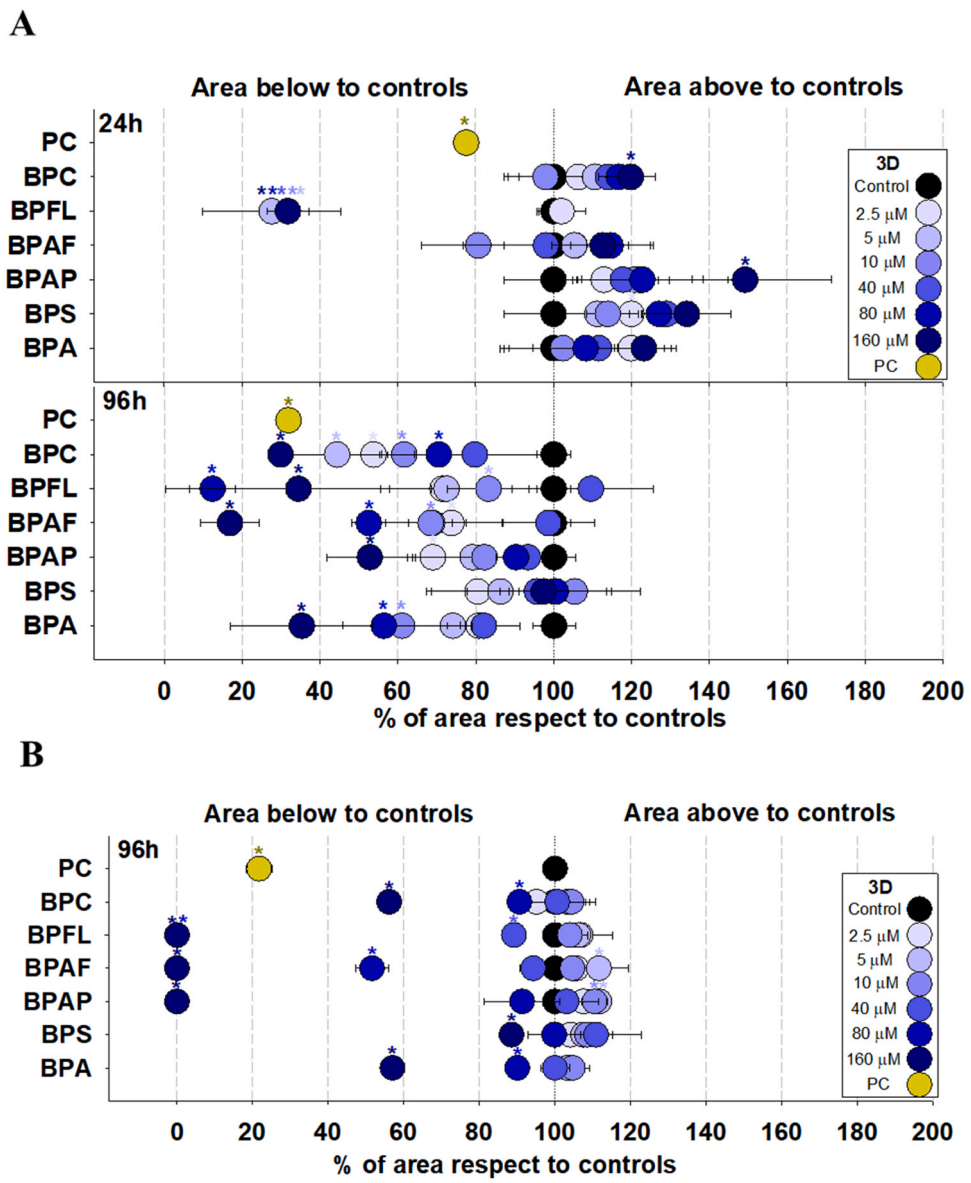

Fig. 3. Percentage of changing area of spheroids respect to controls over BPs exposure (Panel A) and recovery assays (Panel B). Positive control was etoposide at 17 µM. Differences between controls and concentrations of BPs ($p < 0.05$) was analysed by ANOVA with a Dunnett post-hoc (represented with *).

40 and 80 µM with values of 155.81 ± 2.87 and 180.29 ± 30.89% respectively, followed by a decrease to the value of 46.07 ± 0.09% for the concentration of 160 µM. Exposure to BPFL followed the same pattern at 2.5, 10 and 40 µM, whose ROS values were 216.97 ± 72.07, 212.77 ± 61.99 and 220.60 ± 36.02%, respectively, while at higher concentrations, 80 and 160 µM, the values decreased significantly to values of 31.83 ± 10.43 and 29.33 ± 11.71% ($p < 0.05$). Finally, the 2D models exposed to BPC showed values significantly higher than the control from 200–300% at all the concentrations tested ($p < 0.05$).

In the 3D models exposed to BPs over 24 h the trend was different in relation to the 2D models. The spheroids exposed to BPA showed a decrease in ROS of around 50.75 ± 28.17 and 25.83 ± 14.49% for the concentrations of 80 and 160 µM ($p < 0.05$). The BPS analogue produced a significant decrease in concentrations at 40, 80 and 160 µM corresponding to values of 45.82 ± 35.42, 49.06 ± 28.5 and 30.63 ± 5.48% respectively ($p < 0.05$). Regarding BPAP in the 3D model, all the concentrations showed significant decreases of less than 50%, the values were 41.82 ± 32.76 (2.5 µM), 15.88 ± 14.32 (10 µM), 30.73 ± 8.21 (40 µM), 17.72 ± 2.78 (80 µM) and 19.58 ± 4.58% (160 µM) ($p < 0.05$). Exposure to BPFL in the 3D model produced a significant decrease of 36.43 ± 21.28% at 2.5 µM, while at 80 and 160 µM it produced significant increases of around 135% in ROS levels. Finally, the 3D models exposed to BPC showed a significant decrease in all the spheroids exposed to the entire range of concentrations tested with ROS values of around 20–30% compared to the controls ($p < 0.05$).

Regarding the comparison of both in vitro models (2D and 3D), significant differences were found between the models in the acute toxicity tests ($p < 0.05$). The spheroids exposed to BPs tended to decrease in ROS levels, while the 2D model demonstrated significant increases in ROS levels ($p < 0.05$).

After the **chronic toxicity tests** (96 h of exposure to BPs) the trend of the 2D models changed in comparison to the 24 h of exposure to the BPs; Fig. 5. Significant differences ($p < 0.05$) in the ROS percentage were observed after all the exposure to BPs tests. In the 2D models treated with BPA, the same trend as the 24 h exposure was maintained; that is, there were significant differences at 80 and 160 µM with values of 44.62 ± 9.82 and 13.78 ± 3.00% ($p < 0.05$). In the case of BPS there were no significant differences in the 2D model for any of the concentrations studied. Exposure to BPAP presented an increase in ROS with values of 144.81 ± 20.46% at 40 µM, while, at higher concentrations,

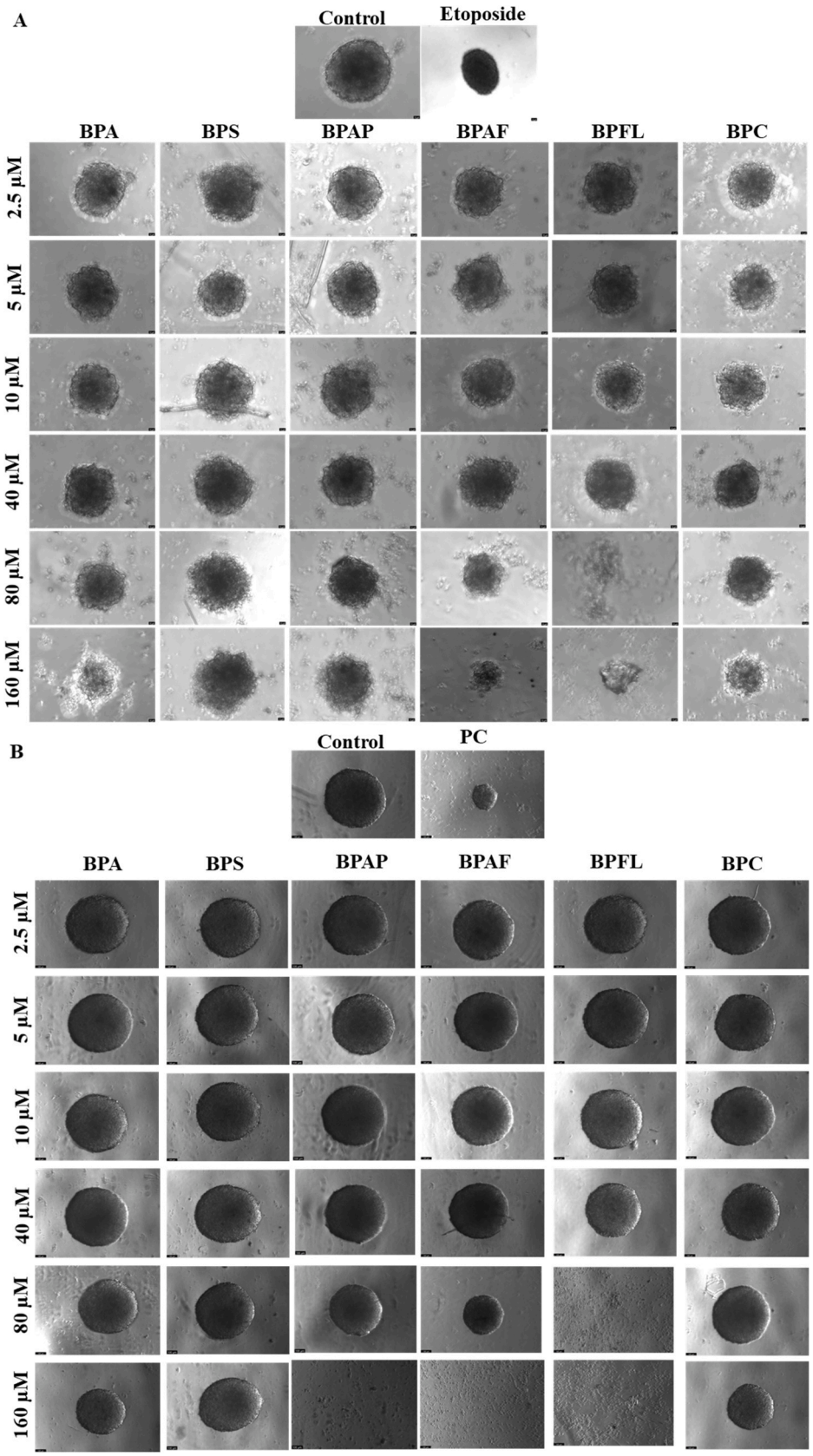

Fig. 4. Microscopy images of spheroids exposed to BPs tested at different concentration over experimental time (96 h of exposure; Panel A) and recovery assays (96 h without BPs exposure; Panel B). Scale 100 µm.

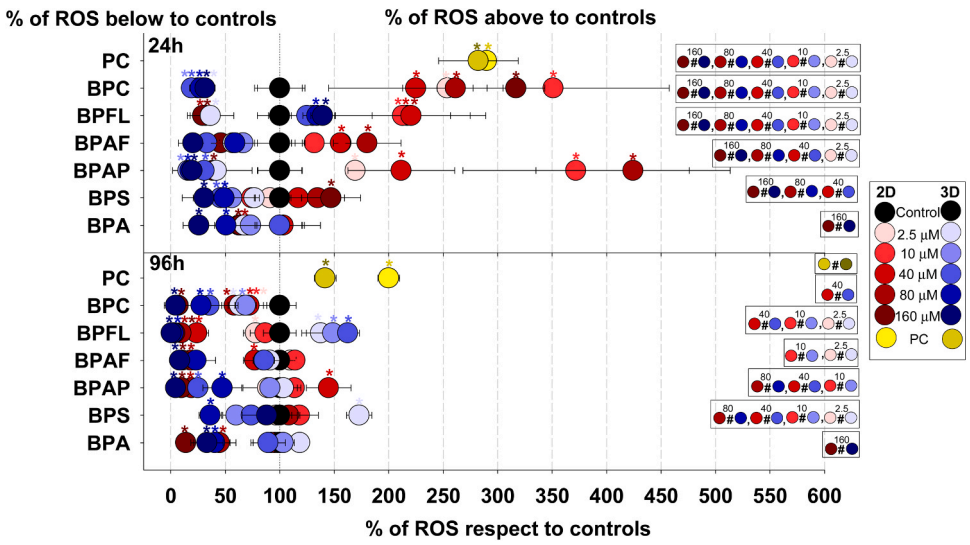

Fig. 5. Percentage of ROS over the BPs exposure time for 2D and 3D models (24 and 96 h, panel A and B respectively). Positive control was etoposide at 17 µM. Differences between controls and concentrations of BPs ($p < 0.05$) was analysed by ANOVA with a Dunnett post-hoc (represented with *). Differences between each in vitro model was study by T-student test (represented with #).

the cells showed a significant decrease in ROS with values of 19.09 ± 11.71 and 9.79 ± 3.03% for 80 and 160 µM, respectively ($p < 0.05$). BPAF exposure in the 2D models showed a decreasing pattern from the concentration of 10 µM at which it presented values from 114.09 ± 3.95% down to 10.55 ± 1.85% for 160 µM ($p < 0.05$). The cultures exposed to BPFL showed significant differences at 2.5, 40, 80 and 160 µM with values of 77.87 ± 11.33, 23.89 ± 10.82, 9.59 ± 7.46 and 3.69 ± 1.32% respectively ($p < 0.05$). Finally, the cells exposed to BPC were the most sensitive when this response was studied, since all the concentrations had significant differences with respect to the controls ($p < 0.05$). The most pronounced decrease began from the concentration of 40 µM with values of 71.93 ± 7.06% decreasing to 58.23 ± 5.69 and 6.87 ± 3.71% at the lowest ones ($p < 0.05$).

In relation to the 3D models, the spheroids exposed to BPA showed a significant decrease with values of 40.42 ± 19.29 and 33.11 ± 14.82% at 80 and 160 µM, respectively ($p < 0.05$). In the case of the exposure to BPS, the only noteworthy 3D model was that of 2.5 and 80 µM with values of 172.92 ± 11.6 and 36.19 ± 10.37%, respectively ($p < 0.05$). In relation to the spheroids exposed to 40, 80 and 160 µM of BPAP, significant differences were observed with values less than 50% compared to the controls ($p < 0.05$). For the spheroids exposed to BPAF, there was a significant decrease at 80 and 160 µM, whose values were 23.24 ± 17.85 and 8.22 ± 4.03% respectively ($p < 0.05$). While the spheroids exposed to BPFL still showed a significant increase in ROS from 2.5 to 40 µM with values higher than 140% ($p < 0.05$); they later decreased to 2.55 ± 2.13% and 0.49 ± 0.04 at 80 and 160 µM respectively ($p < 0.05$). Finally, for the spheroids exposed to BPC, the ROS started to decrease significant from 10–160 µM with values from 68.72 ± 9.84% to 4.45 ± 3.37% ($p < 0.05$).

When comparing both in vitro models (2D and 3D) at 96 h, it was observed that there were significant differences especially in the models treated with BPS, BPAP and BPFL and BPC ($p < 0.05$).

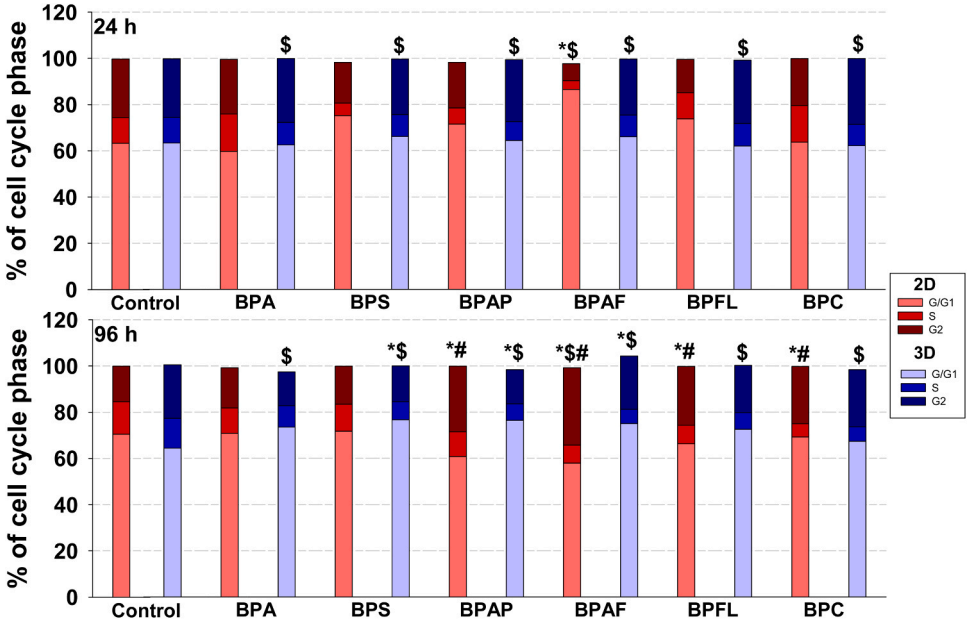

Fig. 6. Percentage of cell cycle phases over the BPs (1 µM) exposure time for 2D and 3D models after 24 and 96 h of exposure. Differences between controls and concentrations of BPs ($p < 0.05$) was analysed by ANOVA with a Dunnett post-hoc (represented with *for phase G0/G1, $ for Phase S and # for phase G2).

3.4. The effects of BPA and its analogues on the cell cycle phases in the 2D and 3D in vitro models

The effect on the cell cycle phases due to exposure to BPs (1 μM) over 24 and 96 h is shown in Fig. 6.

After the acute toxicity test (24 h) in the 2D model, only the cells treated with BPAF showed significant differences in the G0/G1 and S phases, whose values are 86.57 ± 1.01 and 3.72 ± 1.13% respectively compared to the control [63.29 ± 12.66% (G0/G1 phase) and 11.13 ± 2.70% (S phase)]; $p < 0.05$). For the 3D model, the exposure showed significant decreases ($p < 0.05$) in the synthesis phase for all the samples with respect to the controls. The values correspond to 9.67 ± 0.83% for BPA, 9.42 ± 2.14% for BPS, 8.19 ± 1.94% for BPAP, 9.35 ± 0.46% for BPAF, 9.67 ± 0.46% for BPFL and 9.29 ± 0.92% for BPC compared to the control whose value is 13.13 ± 0.66% ($p < 0.05$).

In relation to the **chronic toxicity test** (96 h), for the 2D model, both BPA and BPS did not demonstrate significant differences and maintained similar values to the control. The spheroids treated with BPAP had values of 60.74 ± 0.97 and 28.37 ± 1.2% compared to the controls that were 70.5 ± 3.49 and 15.42 ± 5.34% in phases G0/G1 and G2 ($p < 0.05$), respectively. All the phases were significant for the exposure to BPAF, with values of 57.87 ± 2.36% in the G0/G1 phase, 7.91 ± 0.53% for S and 33.37 ± 2.71% for G2. These values showed a significant reduction compared to the controls with values of 70.50 ± 3.49, 14.02 ± 3.43 and 15.42 ± 5.34% for G0/1 and G2 phases respectively; $p < 0.05$). Finally, exposure to BPFL and the BPC resulted in significant differences in the synthesis phase with values of 7.95 ± 0.03 and 5.6 ± 1.92% respectively with respect to the control values of 14.02 ± 3.43% ($p < 0.05$).

Regarding **chronic exposure** (96 h) in the 3D model, all the samples showed significant differences in the synthesis phase ($p < 0.05$); although these differences were also observed in the G0/G1 phase during exposure to BPS, BPAP and BPAF ($p < 0.05$). In the case of the spheroids exposed to BPA, BPFL and PCB, the values obtained were 9.19 ± 1.61, 7.27 ± 2.17 and 6.36 ± 0.27 compared to the control values with 12.87 ± 1.47% in the S phase ($p < 0.05$). On the other hand, the exposure to BPS, BPAP and BPAF had values of 76.68 ± 2.82, 76.42 ± 1.84 and 75.03 ± 2.96% in the G0/G1 phase and 7.78 ± 1.18, 7.07 ± 1.92 and 6.22 ± 1.37% in the synthesis phase compared to the controls with values of 64.42 ± 3.25% in the G0/G1 phase and 12.87 ± 1.47% in the S phase.

4. Discussion

Despite the increasing concern about the effects of BPA analogues on human health, there are products on the market labelled “BPA free”, nowadays. This label sends a misleading message to the consumers, as it suggests that the product could safe or that BPA analogues are safer alternatives to products with a classical BPA formulation.

Some data have revealed the undesirable effects of BPA analogues. In vivo results have demonstrated that some BPA analogues such as BPAF; BPF and BPS are more toxic than BPA for some model organisms used in toxicology [35–40], for example *Caenorhabditis elegans* (Xiao et al., 2019; Zhou, 2018); and rodents and even humans (Castro et al., 2015; Eladak et al., 2015; LaPlante et al., 2017). However, the adverse effects of BPA and the BPA analogues depend on the system (reproductive toxicity, immunotoxicity and metabolic disorders), the endpoints measured and the taxa studied (McDonough et al., 2021). In relation to in vitro literature, the cytotoxicity and genotoxicity of BPA analogues have been revealed in different cell lines such as hepatocytes; HepG2 (Fic et al., 2013; Hercog et al., 2019; Ozyurt et al., 2022; Sendra et al., 2023; Štampar et al., 2023); stem cells (Harnett et al., 2021); human breast adenocarcinoma cells; MCF-7 (Russo et al., 2019), human cervical epithelial cancer cells; HeLa (Russo et al., 2019) and human breast cancer cells; MDA-kb2 (Ma et al., 2019). Most of the works in vivo and in vitro in the literature have studied the effects of 2 or 3 analogues in comparison to BPA. Therefore, broader studies about BPA analogues and the link between the toxicity/action mechanisms and chemical structure constitute a gap in the knowledge available nowadays. The most studied BPA analogues are BPS, BPF and BPAF, as they are the most common found in the environment (Chen et al., 2016; Liu et al., 2021). However, the sensitivity of chemical analysis and the range of toxicity is not the same for all BPs. Previous studies have revealed that there is a range of BPA analogues that are more toxic than BPA or the other classic BPA analogues studied (Bai et al., 2023; Sendra et al., 2023; Štampar et al., 2023), where a low dose of BPAF and BPFL showed higher genotoxicity and cytotoxicity, respectively, in relation to BPA (Sendra et al., 2023). According to the previous results, the findings of the present work are in line with the previous findings, as the SH-SY5Y cell line showed higher sensitivity to BPFL, BPAF, BPAP and BPC; while BPA and BPS showed the lowest effects or even no-changes with respect to the controls.

Although, some studies have hypothesized that the effects of BPA analogues could be related to the chemical structure (Bai et al., 2023; Gyimah et al., 2022), the results were not clearly evident in the case of BPS. BPS and BPAF are found in the same group as BPs with an unsubstituted phenol ring with a different functional group at the carbon bridge (Zühlke et al., 2020). However, when these two BPA analogues were compared among the other BPA analogues, they are in a different order of toxicity. BPS is found among the less toxic BPA analogues in vivo (Chen et al., 2002; Qiu et al., 2021); and in vitro (Harnett et al., 2021; Hercog et al., 2019; Sendra et al., 2023; Štampar et al., 2023) while BPAF is catalogued among the BPs with higher cytotoxic and genotoxic effects (Chen et al., 2016; Harnett et al., 2021; Sendra et al., 2023).

Adipose tissue has been identified as a significant site for the accumulation of BPA due to its unique ability to store and slowly release hormones and other chemicals over time (Akash et al., 2023). The log Kow of the BPA analogues used in this study were BPFL= 6.08 >BPAP= 4.86 >BPC= 4.74 > BPAF= 4.47 > BPA= 3.32 ->BPS= 1.65. As has been demonstrated previously, higher lipophilicity may induce more severe toxic effects (Bai et al., 2023). Although the main site for the bioaccumulation of BPs is the adipose tissue, it is believed that BPA enters this tissue from the circulatory system (Akash et al., 2023). Therefore, it, and others, could be translocated to immune cells and different organs such as the brain (Chen et al., 2017). Previous findings have suggested that exposure to BPA increases the risk of Alzheimer disease with an increase of APP and the p-tau protein directly related to the abnormal insulin-IR-IRS1 signalling pathway (Wang et al., 2017). In relation to the log Kow values, the present study revealed that BPs with a log Kow ≥ 4 such as BPFL, BPC, BPAP and BPAF can induce more sensitivity in SH-SY5Y than BPs with a log Kow ≤ 4, such as BPA and BPS. Although, clearly the BPs with a log Kow > 4 showed higher sensitivity, the increases in the log Kow were not always correlated with the sensitivity of the endpoint studied.

The human neuroblastoma cell line; SH-SY5Y, when used in toxicology studies, is a target cell line to study the effects and toxicological mechanisms due to its inherent advantages such as autophagy mechanisms, cell death (apoptosis, pyroptosis, or necrosis), oxidative stress, mitochondrial dysfunction, disruption of neurotransmitter homeostasis, and alteration of neuritic length (Lopez-Suarez et al., 2022). Some studies have revealed the sensitivity of the SH-SY5Y cell line to exposure to BPA analogues. In the work of Švajger et al. (Švajger et al., 2016) it was observed that BPF and BPAF affected the formation of dendritic cells. In the work of Nowicki et al. (Nowicki et al., 2016), the BPA uptake, as well as an increase in dopamine transporter levels, effects in tyrosine and insuline routes Tingwei Wang et al. (Wang et al., 2017), GPER-mediated oestrogen signalling (Thesis, 2020), as well as in protein related to immune response (Xiong et al., 2017), neurotoxicity (Ayazgök and Tüylü Küçükkılınç, 2019) were demonstrated and mitochondrial pathways involving ROS (Wang et al., 2021) were also revealed in this cell line exposed to BPA, BPS, BPB. The limited knowledge available concerning the toxicity of different BPA analogues in relation to the

SH-SY5Y cell line was the main purpose for undertaking this work.

However, it is important to bear in mind the limitations of the classical 2D models. The SH-SY5Y cell line derives from a tumour and therefore contains genetic peculiarities that can, potentially, alter the expected response of the cells. Additionally, cell lines do not make it possible to mimic microenvironment perturbations or to test integrative processes (Lopez-Suarez et al., 2022). Furthermore, the nervous system is a highly complex structure with multiple functions such as energy metabolism, calcium homeostasis, electrical activity, synaptogenesis and interactions between neurons. Some authors have improved the 2D models through the differentiation of SH-SY5Y cells in which the mitochondrial function (respiration) appears to be increased (Schneider et al., 2011) and the excitability of the cells, as well as glutamate synthesis are also increased (Heusinkveld and Westerink, 2017; Jantas et al., 2008).

Three-dimensional (3D) models of human-derived cells have recently been extensively used to study disease mechanisms and screen drugs (Duval et al., 2017). Compared to the 2D cultures, these models contain mechanical structural cues and the extracellular microenvironment that mimics physiological conditions (Baker and Chen, 2012). In the case of the SH-SY5Y cell line it has been revealed that the transcriptome of differentiate neurons in a matrigel-based 3D construct differed significantly from the differenced monolayer culture (Li et al., 2022). The mains categories of the KEGG routes that were enriched were: cellular community, membrane transport, replication and repair, neurodegenerative disease, energy metabolism and the nervous system. Furthermore, Gene Set Enrichment Analysis (GSEA) revealed: the enrichment of dopaminergic neuron differentiation, dopaminergic synaptic transmission, extracellular matrix receptor interaction and neuroactive ligand–receptor interaction (Li et al., 2022). Due to these differences between both models; almost 80% of the 2D model results are false positive, when the 2D model is compared to in vivo experiments (Berrouet et al., 2020). Therefore, the improved 3D human models are more relevant with regards to in vivo conditions and could be considered as a practical alternative (Fowler et al., 2012; Gerets et al., 2012; Saleh et al., 2011). The differences in the sensitivity of both models (2D and 3D) were revealed in the present study. The 2D model showed higher sensitivity than the 3D model for the BPs studied in the cell viability assays. Currently, not many studies compare the sensitivity of both in vitro models in the literature (Berrouet et al., 2020; Serras et al., 2021). In the Serras et al. (Serras et al., 2021) review the literature available comparing the sensitivity of different 2D and 3D liver models exposed to paracetamol, diclofenac and troglitazone was assessed. When the IC50 of some endpoints were compared for both models, the review demonstrated that the cell line tested, the growth conditions of the culture and the conditions of the exposure conditioned the IC50 values. The explanation from Berrouet et al. (Berrouet et al., 2020) about the differences in IC50 between the 2D and 3D models in a drug screening were connected to: drug diffusivity, drug action mechanisms, and cell proliferation capabilities. These properties are cues to determine the toxicity dose and could be used to establish limitations in regulatory programmes.

In the present study, the 2D in vitro model showed higher sensitivity than the 3D model in: both exposure times, responses such as cell viability, percentage in area change, percentage of ROS and different phases of the cell cycle. Further, different strategies to respond to the exposure to BPs was observed as there was an increase in ROS in the 2D model and a decrease in ROS in the 3D model at the same concentrations and sampling times. The BPs tested elicited a chronic effect in the endpoints measured. Both in vitro models demonstrated a higher sensitivity after 96 h of exposure, greater in the 3D models, when the results for 24 h were compared with those of 96 h. In the study by Sendra et al., (Sendra et al., 2023) human hepatocyte spheroids also evidenced greater effects during 96 h of exposure in relation to those after 24 h. Despite, both studies [25, and the present study] using the same BPA analogues, concentrations and exposure time, analysing the sensitivity of the cell line revealed the higher sensitivity of SH-SY5Y with respect to the HepG2 cell line. Chronic assays are needed to elucidate the effects provoked, as there is a daily and permanent exposure to BPA and BPA analogues in consumer products, both indoors and outdoors (Chen et al., 2016).

The recovery assays have provided useful information about the resilience or sensitivity of SH-SY5Y spheroids in terms of recovering their viability and the morphology. In relation to cell viability, the recovery time was needed to counteract the previous exposure to the BPs (except for BPFL where the cell viability was lower, and for BPS no significant effects were found), where more than 20% of cell viability was recovered with regard to the chronic assays (96 h). Although cell viability was recovered in most cases, the spheroids could not maintain their morphology. In this way the 3D model could lose the representativeness of spheroids as an organ or tissue, while the 2D cells maintain a proliferative capacity. The spheroids exposed to BPA and BPC were able to recover their area and shape for all the concentrations tested in relation to chronic exposure. This could be indicative of a partial or total recovery if the exposure to these BPs ceased. On the other hand, the recovery of the area only occurred for doses from 2.5–40 μM for BPs such as BPFL, BPAP and BPAF. However, at higher doses the structure was lost. This means, that mechanisms such as replication and proliferation were recovered, while the mechanisms responsible for maintaining the morphology of the spheroids could be negatively affected by previous chronic exposure. Some results have demonstrated that proteins related to cell junctions and the extracellular matrix are also known to be involved in the control of cell proliferation and these two related mechanisms are complex (Zaidan Dagli and Hernandez-Blazquez, 2007). However, this relation was not observed under chronic exposure for some of the BPs.

Exposure to these BPs not only provoked cytotoxicity but also genotoxicity, which was studied by analysing the cell cycle. Significant changes were observed at 1 μM, such as was observed in the HepG2 spheroids for this endpoint and different genotoxic responses were recorded (Sendra et al., 2023). In the work by Senyildiz et al. (Senyildiz et al., 2017), DNA methylation and global levels of H3K9me3, H3K9ac and H3K4me3 histone modifications were observed at 10 μM of BPA for 96 h. In addition, alterations to the regulation of chromatin modifying genes were also observed and these may be used as bioindicators of the genotoxicity of BPs (Senyildiz et al., 2017).

5. Conclusions

The toxic effects of BPA and the BPA analogues (BPS, BPAP, BPAF, BPFL and BPC) in neuroblastoma cell line have been revealed in this work. The BPs tested, except for BPS, do not represent safer alternatives to the classic BPA. Among the BPA analogues tested; BPFL, BPAF, BPAP and BPC were actually shown to be more toxic than BPS and BPA. This study has demonstrated that these BPA analogues triggered a higher toxicity response after a chronic exposure in comparison to an acute exposure. These results are relevant because a low dose of BPA analogues maintained over time could provoke irreversible effects. Although chronic exposure provoked unwanted effects, after a recovery time of 96 h the spheroids were able to recover their cell viability and morphology except for the spheroids previously exposed to the highest concentration of BPFL, BPAF and BPAP for 96 h.

2D and 3D SH-SY5Y models were compared to evaluate the potential of 3D cell culture as an alternative in vitro model to test neurotoxicological chemical compounds. The dimensionality of the 3D models provides functions mimicking the in vivo model. The performance of the 3D SH-SY5Y model in this work could be applied in environmental toxicity testing as an alternative to non-representative 2D models.

Funding

This study has been funded by Juan de la Cierva Incorporación (IJC

2020–043162-I) contract funded by MCIN/AEI/10.13039/501100011033, European Union NextGeneration EU/PRTR.

CRediT authorship contribution statement

Múñiz Pilar: Writing – review & editing, Resources. **Cavia-Saiz Mónica:** Writing – review & editing. **Sendra Marta:** Writing – original draft, Methodology, Investigation, Formal analysis, Data curation, Conceptualization.

Declaration of Competing Interest

The authors declare that they have no known competing financial interests or personal relationships that could have appeared to influence the work reported in this paper.

Data availability

Data will be made available on request.

Acknowledgment

Marta Sendra thanks to the Juan de la Cierva Incorporación (IJC 2020–043162-I) contract funded by MCIN/AEI/10.13039/501100011033, European Union NextGenerationEU/PRTR. The authors are grateful to Natalia Gallo for her support in the Lab facilities.

References

Akash, M.S.H., Fatima, M., Rehman, K., Rehman, Q., Chauhdary, Z., Nadeem, A., Mir, T. M., 2023. Resveratrol mitigates bisphenol a-induced metabolic disruptions: insights from experimental studies. Molecules 28, 1–23. https://doi.org/10.3390/molecules28155865.

Ayazgök, B., Tüylü Küçükkılınç, T., 2019. Low-dose bisphenol A induces RIPK1-mediated necroptosis in SH-SY5Y cells: Effects on TNF-α and acetylcholinesterase. J. Biochem. Mol. Toxicol. 33, 1–7. https://doi.org/10.1002/jbt.22233.

Bai, C., Zheng, Y., Tian, L., Lin, J., Song, Y., Huang, C., Dong, Q., Chen, J., 2023. Structure-based developmental toxicity and ASD-phenotypes of bisphenol A analogues in embryonic zebrafish. Ecotoxicol. Environ. Saf. 253, 114643 https://doi.org/10.1016/j.ecoenv.2023.114643.

Baker, B.M., Chen, C.S., 2012. Deconstructing the third dimension-how 3D culture microenvironments alter cellular cues. J. Cell Sci. 125, 3015–3024. https://doi.org/10.1242/jcs.079509.

Barber, L.B., 2013. 1.13 Emerging Contaminants. Comprehensive Water Quality and Purification. Elsevier Ltd,. https://doi.org/10.1016/B978-0-12-382182-9.00015-3.

Bell, C.C., Hendriks, D.F.G., Moro, S.M.L., Ellis, E., Walsh, J., Renblom, A., Fredriksson Puigvert, L., Dankers, A.C.A., Jacobs, F., Snoeys, J., Sison-Young, R.L., Jenkins, R.E., Nordling, Å., Mkrtchian, S., Park, B.K., Kitteringham, N.R., Goldring, C.E.P., Lauschke, V.M., Ingelman-Sundberg, M., 2016. Characterization of primary human hepatocyte spheroids as a model system for drug-induced liver injury, liver function and disease. Sci. Rep. 6, 1–13. https://doi.org/10.1038/srep25187.

Berrouet, C., Dorilas, N., Rejniak, K.A., Tuncer, N., 2020. Comparison of Drug Inhibitory Effects (IC 50) in Monolayer and Spheroid Cultures. Bull. Math. Biol. 82, 1–23. https://doi.org/10.1007/s11538-020-00746-7.

Bi, N., Gu, X., Fan, A., Li, D., Wang, M., Zhou, R., Sun, Q.C., Wang, H.L., 2022. Bisphenol-A exposure leads to neurotoxicity through upregulating the expression of histone deacetylase 2 in vivo and in vitro. Toxicology 465, 153052. https://doi.org/10.1016/j.tox.2021.153052.

Castro, B., Sánchez, P., Torres, J.M., Ortega, E., 2015. Bisphenol A, bisphenol F and bisphenol S affect differently 5α-reductase expression and dopamine-serotonin systems in the prefrontal cortex of juvenile female rats. Environ. Res. 142, 281–287. https://doi.org/10.1016/j.envres.2015.07.001.

Chen, D., Kannan, K., Tan, H., Zheng, Z., Feng, Y.L., Wu, Y., Widelka, M., 2016. Bisphenol Analogues Other Than BPA: Environmental Occurrence, Human Exposure, and Toxicity - A Review. Environ. Sci. Technol. 50, 5438–5453. https://doi.org/10.1021/acs.est.5b05387.

Chen, M.Y., Ike, M., Fujita, M., 2002. Acute toxicity, mutagenicity, and estrogenicity of bisphenol-A and other bisphenols. Environ. Toxicol. 17, 80–86. https://doi.org/10.1002/tox.10035.

Chen, Q., Yin, D., Jia, Y., Schiwy, S., Legradi, J., Yang, S., Hollert, H., 2017. Enhanced uptake of BPA in the presence of nanoplastics can lead to neurotoxic effects in adult zebrafish. Sci. Total Environ. 609, 1312–1321. https://doi.org/10.1016/j.scitotenv.2017.07.144.

Czarny-Krzymińska, K., Krawczyk, B., Szczukocki, D., 2022. Toxicity of bisphenol A and its structural congeners to microalgae Chlorella vulgaris and Desmodesmus armatus. J. Appl. Phycol. 34, 1397–1410. https://doi.org/10.1007/s10811-022-02704-3.

Duval, K., Grover, H., Han, L.H., Mou, Y., Pegoraro, A.F., Fredberg, J., Chen, Z., 2017. Modeling physiological events in 2D vs. 3D cell culture. Physiology 32, 266–277. https://doi.org/10.1152/physiol.00036.2016.

EFSA EMA, 2023, Report on divergent views between EFSA and EMA on EFSA ' s updated bisphenol A assessment 1–8.

Eilenberger, C., Rothbauer, M., Ehmoser, E.K., Ertl, P., Küpcü, S., 2019. Effect of Spheroidal Age on Sorafenib Diffusivity and Toxicity in a 3D HepG2 Spheroid Model. Sci. Rep. 9, 1–11. https://doi.org/10.1038/s41598-019-41273-3.

Eladak, S., Grisin, T., Moison, D., Guerquin, M.J., N'Tumba-Byn, T., Pozzi-Gaudin, S., Benachi, A., Livera, G., Rouiller-Fabre, V., Habert, R., 2015. A new chapter in the bisphenol a story: Bisphenol S and bisphenol F are not safe alternatives to this compound. Fertil. Steril. 103, 11–21. https://doi.org/10.1016/j.fertnstert.2014.11.005.

Fic, A., Žegura, B., Sollner Dolenc, M., Filipič, M., Peterlin Mašič, L., 2013. Mutagenicity and DNA damage of bisphenol a and its structural analogues in HepG2 cells. Arh. Hig. Rada Toksikol. 64, 189–200. https://doi.org/10.2478/10004-1254-64-2013-2319.

Fowler, P., Smith, R., Smith, K., Young, J., Jeffrey, L., Kirkland, D., Pfuhler, S., Carmichael, P., 2012. Reduction of misleading (" false") positive results in mammalian cell genotoxicity assays. II. Importance of accurate toxicity measurement. Mutat. Res. - Genet. Toxicol. Environ. Mutagen. 747, 104–117. https://doi.org/10.1016/j.mrgentox.2012.04.013.

Gerets, H.H.J., Tilmant, K., Gerin, B., Chanteux, H., Depelchin, B.O., Dhalluin, S., Atienzar, F.A., 2012. Characterization of primary human hepatocytes, HepG2 cells, and HepaRG cells at the mRNA level and CYP activity in response to inducers and their predictivity for the detection of human hepatotoxins. Cell Biol. Toxicol. 28, 69–87. https://doi.org/10.1007/s10565-011-9208-4.

González, N., Cunha, S.C., Ferreira, R., Fernandes, J.O., Marquès, M., Nadal, M., Domingo, J.L., 2020. Concentrations of nine bisphenol analogues in food purchased from Catalonia (Spain): Comparison of canned and non-canned foodstuffs. Food Chem. Toxicol. 136, 110992 https://doi.org/10.1016/j.fct.2019.110992.

Gyimah, E., Zhu, X., Zhang, Ziqi, Guo, M., Xu, H., Mensah, J.K., Dong, X., Zhang, Zhen, Gyimah, G.N.W., 2022. Oxidative Stress and Apoptosis in Bisphenol AF–Induced Neurotoxicity in Zebrafish Embryos. Environ. Toxicol. Chem. 41, 2273–2284. https://doi.org/10.1002/etc.5412.

Harnett, K.G., Chin, A., Schuh, S.M., 2021. BPA and BPA alternatives BPS, BPAF, and TMBPF, induce cytotoxicity and apoptosis in rat and human stem cells. Ecotoxicol. Environ. Saf. 216 https://doi.org/10.1016/j.ecoenv.2021.112210.

Hercog, K., Maisanaba, S., Filipič, M., Sollner-Dolenc, M., Kač, L., Žegura, B., 2019. Genotoxic activity of bisphenol A and its analogues bisphenol S, bisphenol F and bisphenol AF and their mixtures in human hepatocellular carcinoma (HepG2) cells. Sci. Total Environ. 687, 267–276. https://doi.org/10.1016/j.scitotenv.2019.05.486.

Heusinkveld, H.J., Westerink, R.H.S., 2017. Comparison of different in vitro cell models for the assessment of pesticide-induced dopaminergic neurotoxicity. Toxicol Vitr. 45, 81–88. https://doi.org/10.1016/j.tiv.2017.07.030.

Hyun, S.A., Ko, M.Y., Jang, S., Lee, B.S., Rho, J., Kim, K.K., Kim, W.Y., Ka, M., 2022. Bisphenol-A impairs synaptic formation and function by RGS4-mediated regulation of BDNF signaling in the cerebral cortex. DMM Dis. Model. Mech. 15 https://doi.org/10.1242/dmm.049177.

Ikhlas, S., Usman, A., Ahmad, M., 2019. In vitro study to evaluate the cytotoxicity of BPA analogues based on their oxidative and genotoxic potential using human peripheral blood cells. Toxicol. Vitr. 60, 229–236. https://doi.org/10.1016/j.tiv.2019.06.001.

Jantas, D., Pytel, M., Mozrzymas, J.W., Leskiewicz, M., Regulska, M., Antkiewicz-Michaluk, L., Lason, W., 2008. The attenuating effect of memantine on staurosporine-, salsolinol- and doxorubicin-induced apoptosis in human neuroblastoma SH-SY5Y cells. Neurochem. Int. 52, 864–877. https://doi.org/10.1016/j.neuint.2007.10.003.

LaPlante, C.D., Catanese, M.C., Bansal, R., Vandenberg, L.N., 2017. Bisphenol S alters the lactating mammary gland and nursing behaviors in mice exposed during pregnancy and lactation. Endocrinology 158, 3448–3461. https://doi.org/10.1210/en.2017-00437.

Lee, S., Kim, C., Youn, H., Choi, K., 2017. Thyroid hormone disrupting potentials of bisphenol A and its analogues - in vitro comparison study employing rat pituitary (GH3) and thyroid follicular (FRTL-5) cells. Toxicol. Vitr. 40, 297–304. https://doi.org/10.1016/j.tiv.2017.02.004.

Li, C., Sang, C., Zhang, Shuo, Zhang, Sai, Gao, H., 2023. Effects of bisphenol A and bisphenol analogs on the nervous system. Chin. Med. J. (Engl.). 136, 295–304. https://doi.org/10.1097/CM9.0000000000002170.

Li, Z.F., Cui, L., Jin, M.M., Hu, D.Y., Hou, X.G., Liu, S.S., Zhang, X., Zhu, J.H., 2022. A Matrigel-based 3D construct of SH-SY5Y cells models the α-synuclein pathologies of Parkinson's disease. DMM. Dis. Model. Mech. 15 https://doi.org/10.1242/dmm.049125.

Liu, J., Zhang, L., Lu, G., Jiang, R., Yan, Z., Li, Y., 2021. Occurrence, toxicity and ecological risk of Bisphenol A analogues in aquatic environment – A review. Ecotoxicol. Environ. Saf. 208 https://doi.org/10.1016/j.ecoenv.2020.111481.

Liu, M., Jia, S., Dong, T., Han, Y., Xue, J., Wanjaya, E.R., Fang, M., 2019. The occurrence of bisphenol plasticizers in paired dust and urine samples and its association with oxidative stress. Chemosphere 216, 472–478. https://doi.org/10.1016/j.chemosphere.2018.10.090.

Lopez-Suarez, L., Awabdh, S.Al, Coumoul, X., Chauvet, C., 2022. The SH-SY5Y human neuroblastoma cell line, a relevant in vitro cell model for investigating neurotoxicology in human: Focus on organic pollutants. Neurotoxicology 92, 131–155. https://doi.org/10.1016/j.neuro.2022.07.008.

Lucarini, F., Krasniqi, T., Bailat Rosset, G., Roth, N., Hopf, N.B., Broillet, M.-C., Staedler, D., 2020. Exposure to New Emerging Bisphenols Among Young Children in

Switzerland. : Int. J. Environ. Res. Public Health MDPI AG 4793. https://doi.org/10.3390/ijerph17134793.
Lv, Y., Rui, C., Dai, Y., Pang, Q., Li, Y., Fan, R., Lu, S., 2016. Exposure of children to BPA through dust and the association of urinary BPA and triclosan with oxidative stress in Guangzhou, China. Environ. Sci. Process. Impacts 18, 1492–1499. https://doi.org/10.1039/c6em00472e.
Ma, Y., Liu, H., Wu, J., Yuan, L., Wang, Y., Du, X., Wang, R., Marwa, P.W., Petlulu, P., Chen, X., Zhang, H., 2019. The adverse health effects of bisphenol A and related toxicity mechanisms. Environ. Res. 176 https://doi.org/10.1016/j.envres.2019.108575.
McDonough, C.M., Xu, H.S., Guo, T.L., 2021. Toxicity of bisphenol analogues on the reproductive, nervous, and immune systems, and their relationships to gut microbiome and metabolism: insights from a multi-species comparison. Crit. Rev. Toxicol. 51, 283–300. https://doi.org/10.1080/10408444.2021.1908224.
Miodovnik, A., Engel, S.M., Zhu, C., Ye, X., Soorya, L.V., Silva, M.J., Calafat, A.M., Wolff, M.S., 2011. Endocrine disruptors and childhood social impairment. Neurotoxicology 32, 261–267. https://doi.org/10.1016/j.neuro.2010.12.009.
Ni, Y., Hu, L., Yang, S., Ni, L., Ma, L., Zhao, Y., Zheng, A., Jin, Y., Fu, Z., 2021. Bisphenol A impairs cognitive function and 5-HT metabolism in adult male mice by modulating the microbiota-gut-brain axis. Chemosphere 282, 130952. https://doi.org/10.1016/j.chemosphere.2021.130952.
Nowicki, B.A., Hamada, M.A., Robinson, G.Y., Jones, D.C., 2016. Adverse effects of bisphenol A (BPA) on the dopamine system in two distinct cell models and corpus striatum of the Sprague-Dawley rat. J. Toxicol. Environ. Heal. - Part A Curr. Issues 79, 912–924. https://doi.org/10.1080/15287394.2016.1204577.
Ozyurt, B., Ozkemahli, G., Yirun, A., Ozyurt, A.B., Bacanli, M., Basaran, N., Kocer-Gumusel, B., Erkekoglu, P., 2022. Comparative evaluation of the effects of bisphenol derivatives on oxidative stress parameters in HepG2 cells. Drug Chem. Toxicol. 0, 1–9. https://doi.org/10.1080/01480545.2022.2028823.
Perera, F., Nolte, E.L.R., Wang, Y., Margolis, A.E., Calafat, A.M., Wang, S., Garcia, W., Hoepner, L.A., Peterson, B.S., Rauh, V., Herbstman, J., 2016. Bisphenol A exposure and symptoms of anxiety and depression among inner city children at 10–12 years of age. Environ. Res. 151, 195–202. https://doi.org/10.1016/j.envres.2016.07.028.
Pfuhler, S., van Benthem, J., Curren, R., Doak, S.H., Dusinska, M., Hayashi, M., Heflich, R.H., Kidd, D., Kirkland, D., Luan, Y., Ouedraogo, G., Reisinger, K., Sofuni, T., van Acker, F., Yang, Y., Corvi, R., 2020. Use of in vitro 3D tissue models in genotoxicity testing: Strategic fit, validation status and way forward. Report of the working group from the 7th International Workshop on Genotoxicity Testing (IWGT), 503135 Mutat. Res. - Genet. Toxicol. Environ. Mutagen 850–851. https://doi.org/10.1016/j.mrgentox.2020.503135.
Pradhan, L.K., Sarangi, P., Sahoo, P.K., Kundu, S., Chauhan, N.R., Kumar Das, S., 2023. Bisphenol A-induced neurobehavioral transformation is associated with augmented monoamine oxidase activity and neurodegeneration in zebrafish brain. Environ. Toxicol. Pharmacol. 97, 104027 https://doi.org/10.1016/j.etap.2022.104027.
Qiu, W., Liu, S., Chen, H., Luo, S., Xiong, Y., Wang, X., Xu, B., Zheng, C., Wang, K.J., 2021. The comparative toxicities of BPA, BPB, BPS, BPF, and BPAF on the reproductive neuroendocrine system of zebrafish embryos and its mechanisms. J. Hazard. Mater. 406, 124303 https://doi.org/10.1016/j.jhazmat.2020.124303.
Rezg, R., El-Fazaa, S., Gharbi, N., Mornagui, B., 2014. Bisphenol A and human chronic diseases: Current evidences, possible mechanisms, and future perspectives. Environ. Int. 64, 83–90. https://doi.org/10.1016/j.envint.2013.12.007.
Russo, G., Barbato, F., Mita, D.G., Grumetto, L., 2019. Occurrence of Bisphenol A and its analogues in some foodstuff marketed in Europe. Food Chem. Toxicol. 131 https://doi.org/10.1016/j.fct.2019.110575.
Saleh, F.A., Whyte, M., Genever, P.G., 2011. Effects of endothelial cells on human mesenchymal stem cell activity in a three-dimensional in vitro model. Eur. Cells Mater. 22, 242–257. https://doi.org/10.22203/eCM.v022a19.
Schneider, L., Giordano, S., Zelickson, B.R., Johnson, S., M, A., Benavides, G., Ouyang, X., Fineberg, N., Darley-Usmar, V.M., Zhang, J., 2011. Differentiation of SH-SY5Y cells to a neuronal phenotype changes cellular bioenergetics and the response to oxidative stress. Free Radic. Biol. Med. 51, 2007–2017. https://doi.org/10.1016/j.freeradbiomed.2011.08.030.
Sendra, M., Stampar, M., Fras, K., Novoa, B., Figueras Huerta, A., Zegura, B., 2023. Adverse (geno)toxic effects of bisphenol A and its analogues in hepatic 3D cell model. Environ. Int. 171, 107721 https://doi.org/10.1016/j.envint.2022.107721.
Senyildiz, M., Karaman, E.F., Bas, S.S., Pirincci, P.A., Ozden, S., 2017. Effects of BPA on global DNA methylation and global histone 3 lysine modifications in SH-SY5Y cells: An epigenetic mechanism linking the regulation of chromatin modifiying genes. Toxicol Vitr. 44, 313–321. https://doi.org/10.1016/j.tiv.2017.07.028.
Serras, A.S., Rodrigues, J.S., Cipriano, M., Rodrigues, A.V., Oliveira, N.G., Miranda, J.P., 2021. A Critical Perspective on 3D Liver Models for Drug Metabolism and Toxicology Studies. Front. Cell Dev. Biol. 9, 1–30. https://doi.org/10.3389/fcell.2021.626805.
Sevastre-Berghian, A.C., Casandra, C., Gheban, D., Olteanu, D., Olanescu Vaida Voevod, M.C., Rogojan, L., Filip, G.A., Bâldea, I., 2022. Neurotoxicity of Bisphenol A and the Impact of Melatonin Administration on Oxidative Stress, ERK/NF-kB Signaling Pathway, and Behavior in Rats. Neurotox. Res. 40, 1882–1894. https://doi.org/10.1007/s12640-022-00618-z.
Štampar, M., Ravnjak, T., Domijan, A.M., Žegura, B., 2023. Combined Toxic Effects of BPA and Its Two Analogues BPAP and BPC in a 3D HepG2 Cell Model. Molecules 28. https://doi.org/10.3390/molecules28073085.
Štampar, M., Sedighi Frandsen, H., Rogowska-Wrzesinska, A., Wrzesinski, K., Filipič, M., Žegura, B., 2021. Hepatocellular carcinoma (HepG2/C3A) cell-based 3D model for genotoxicity testing of chemicals. Sci. Total Environ. 755 https://doi.org/10.1016/j.scitotenv.2020.143255.
Štampar, M., Tomc, J., Filipič, M., Žegura, B., 2019. Development of in vitro 3D cell model from hepatocellular carcinoma (HepG2) cell line and its application for genotoxicity testing. Arch. Toxicol. 93, 3321–3333. https://doi.org/10.1007/s00204-019-02576-6.
Štampar, M., Žabkar, S., Filipič, M., Žegura, B., 2022. HepG2 spheroids as a biosensor-like cell-based system for (geno)toxicity assessment. Chemosphere 291. https://doi.org/10.1016/j.chemosphere.2021.132805.
Sun, Y., Nakashima, M.N., Takahashi, M., Kuroda, N., Nakashima, K., 2002. Determination of bisphenol A in rat brain by microdialysis and column switching high-performance liquid chromatrography with fluorescence detection. Biomed. Chromatogr. 16, 319–326. https://doi.org/10.1002/bmc.161.
Švajger, U., Dolenc, M.S., Jeras, M., 2016. In vitro impact of bisphenols BPA, BPF, BPAF and 17β-estradiol (E2) on human monocyte-derived dendritic cell generation, maturation and function. Int. Immunopharmacol. 34, 146–154. https://doi.org/10.1016/j.intimp.2016.02.030.
Takahashi, M., Komada, M., Miyazawa, K., Goto, S., Ikeda, Y., 2018. Bisphenol A exposure induces increased microglia and microglial related factors in the murine embryonic dorsal telencephalon and hypothalamus. Toxicol. Lett. 284, 113–119. https://doi.org/10.1016/j.toxlet.2017.12.010.
Thesis, A., 2020, The Effects of Bisphenol-A and its Analogs on Neuronal Oestrogen Sensitive Kinase Pathways.
Thoene, M., Rytel, L., Nowicka, N., Wojtkiewicz, J., 2018. The state of bisphenol research in the lesser developed countries of the EU: A mini-review. Toxicol. Res. (Camb.). 7, 371–380. https://doi.org/10.1039/c8tx00064f.
Wang, C., He, J., Xu, T., Han, H., Zhu, Z., Meng, L., Pang, Q., Fan, R., 2021. Bisphenol A (BPA), BPS and BPB-induced oxidative stress and apoptosis mediated by mitochondria in human neuroblastoma cell lines. Ecotoxicol. Environ. Saf. 207, 111299 https://doi.org/10.1016/j.ecoenv.2020.111299.
Wang, T., Xie, C., Yu, P., Fang, F., Zhu, J., Cheng, J., Gu, A., Wang, J., Xiao, H., 2017. Involvement of insulin signaling disturbances in bisphenol a-induced Alzheimer's disease-like neurotoxicity. Sci. Rep. 7, 1–12. https://doi.org/10.1038/s41598-017-07544-7.
Xiao, X., Zhang, X., Zhang, C., Li, J., Zhao, Y., Zhu, Y., Zhang, J., Zhou, X., 2019. Toxicity and multigenerational effects of bisphenol S exposure to: Caenorhabditis elegans on developmental, biochemical, reproductive and oxidative stress. Toxicol. Res. (Camb.). 8, 630–640. https://doi.org/10.1039/c9tx00055k.
Xiong, S., Wang, Y., Li, H., Zhang, X., 2017. Low Dose of Bisphenol A Activates NF-κB/IL-6 Signals to Increase Malignancy of Neuroblastoma Cells. Cell. Mol. Neurobiol. 37, 1095–1103. https://doi.org/10.1007/s10571-016-0443-3.
Zaidan Dagli, M.L., Hernandez-Blazquez, F.J., 2007. Roles of gap junctions and connexins in non-neoplastic pathological processes in which cell proliferation is involved. J. Membr. Biol. 218, 79–91. https://doi.org/10.1007/s00232-007-9045-9.
Zhou, D., 2018. Ecotoxicity of bisphenol S to Caenorhabditis elegans by prolonged exposure in comparison with bisphenol A. Environ. Toxicol. Chem. 37, 2560–2565. https://doi.org/10.1002/etc.4214.
Zühlke, M.K., Schlüter, R., Mikolasch, A., Henning, A.K., Giersberg, M., Lalk, M., Kunze, G., Schweder, T., Urich, T., Schauer, F., 2020. Biotransformation of bisphenol A analogues by the biphenyl-degrading bacterium Cupriavidus basilensis - a structure-biotransformation relationship. Appl. Microbiol. Biotechnol. 104, 3569–3583. https://doi.org/10.1007/s00253-020-10406-4.